

Converting ECG Signals to Images for Efficient Image-text Retrieval via Encoding

Jielin Qiu^{*1}

Jiacheng Zhu^{*1}

Shiqi Liu¹

William Han¹

Jingqi Zhang¹

Chaojing Duan²

Michael A. Rosenberg³

Emerson Liu²

Douglas Weber¹

Ding Zhao¹

¹ Carnegie Mellon University

² Allegheny Health Network

³ University of Colorado Denver - Anschutz Medical Campus

* marked as equal contribution

JIELINQ@ANDREW.CMU.EDU

JZHU4@ANDREW.CMU.EDU

SHIQILIU@ANDREW.CMU.EDU

WILLHAN327@GMAIL.COM

JINGQIZ@ANDREW.CMU.EDU

CHAOJIND@ANDREW.CMU.EDU

MICHAEL.A.ROSENBERG@CUANSCHUTZ.EDU

EMERSONLIU@MSN.COM

DOUGWEBER@CMU.EDU

DINGZHAO@CMU.EDU

Abstract

Automated interpretation of electrocardiograms (ECG) has garnered significant attention with the advancements in machine learning methodologies. Despite the growing interest in automated ECG interpretation using machine learning, most current studies focus solely on classification or regression tasks and overlook a crucial aspect of clinical cardio-disease diagnosis: the diagnostic report generated by experienced human clinicians. In this paper, we introduce a novel approach to ECG interpretation, leveraging recent breakthroughs in Large Language Models (LLMs) and Vision-Transformer (ViT) models. Rather than treating ECG diagnosis as a classification or regression task, we propose an alternative method of automatically identifying the most similar clinical cases based on the input ECG data. Also, since interpreting ECG as images are more affordable and accessible, we process ECG as encoded images and adopt a vision-language learning paradigm to jointly learn vision-language alignment between encoded ECG images and ECG diagnosis reports. Encoding ECG into images can result in an efficient ECG retrieval system, which will be highly practical and useful in clinical applications. More importantly, our findings could serve as a crucial resource for providing diagnostic services in regions where only paper-printed ECG images are accessible due to past underdevelopment.

1. Introduction

Cardiovascular diseases, such as heart attacks and strokes, account for the majority of global deaths. Electrocardiogram (ECG) is a vital tool in cardiology and electrophysiology, as it provides valuable information about the heart's structure, electrical activity, and potential systemic conditions through waveform changes in timing and morphology. Accurate interpretation of clinical ECGs is critical, as it remains a primary method for identifying cardiac abnormalities and screening populations at risk of heart-related issues.

The precise interpretation of electrocardiograms (ECGs) is essential for providing timely, efficient, and cost-effective interventions for acute cardiac conditions. Therefore, using reliable machine learning algorithms to assist in ECG interpretations can significantly impact patient outcomes; these studies have covered a range of topics, including deep learning classification (Nonaka and Seita, 2021; Khurshid et al., 2021; Raghunath et al., 2021; Giudicessi et al., 2021; Strodthoff et al., 2021), adversarial attack (Han et al., 2020a; Hossain et al., 2021; Chen et al., 2020a), data augmentation (Raghu et al., 2022; Nonaka and Seita, 2020), contrastive learning (Gopal et al., 2021), and the application of transformer models (Che et al., 2021; Natarajan et al., 2020; Behinaein et al., 2021; Song et al., 2021).

However, there are limitations to most existing ML ECG interpretation frameworks due to practical reasons. First of all, the vast majority of current machine learning approaches in ECG analysis solely utilize the ECG signal as input and the diagnosis outcome as a label, so as to adapt it to the supervised learning paradigm, as commonly done in other domains such as computer vision and natural language processing. However, the diagnosis and interpretation of ECG is a multifaceted process (Guglin and Thatai, 2006) that involves a more intricate hierarchy of disorders. For example, the ST/T changes superclass can further be divided into subclasses, including ischemic in anterior leads (ISCA), ischemic in inferior leads (ISCI), non-specific ischemic (ISC), and non-specific ST changes (NST). In practice, physicians often provide a comprehensive report (Wagner et al., 2020) to capture the nuanced features of the ECG signal along with a categorical diagnosis. On the other hand, AI-empowered ECG interpretation frameworks assume the existence of an advanced information system that allows for the digitized processing of ECG data. In reality, patients and doctors primarily leverage paper-printed ECGs (Zhang et al., 2023) collected by ECG monitor machines (Olson et al., 2013). More importantly, the paper-printed ECG images are the only protocols in **underdeveloped regions**.

To overcome the limitations outlined above, we aim to advance the automation of ECG interpretation by tackling the following challenge: Given a raw ECG image as input, *can we automatically match it with the most similar ECG records in the database*, by leveraging joint inference of the correspondence between the ECG signal and the expert-written report?

The aforementioned functionality can prove to be a highly effective tool for aiding in the diagnosis of common diseases, such as arrhythmia (Hong et al., 2020; Fu et al., 2021), thereby decreasing the workload of physicians (Hannun et al., 2019). Moreover, such an ECG data retrieval system can help in diagnosing complex conditions such as atrial fibrillation and contractile dysfunction (Attia et al., 2019b,a), which are challenging for supervised learning networks due to the rarity in training data samples. Conversely, the retrieval system can accurately identify similar ECG records by utilizing a multimodal similarity score.

Fortunately, relating the corresponding data among different modalities is an actively researched topic in other areas, such as computer vision and natural language processing. Specifically, cross-modal image-text retrieval (ITR) (Li et al., 2021a) aims to retrieve relevant samples from one modality based on input from another modality. Thanks to the rise of large pretrained models such as BERT (Devlin et al., 2019b) and CLIP (Radford et al., 2021b), transformer-based models have accelerated the development of this topic.

To achieve this, we propose an ECG-Text retrieval system that can automatically retrieve expert-written reports and corresponding ECG records using a multimodal information retrieval framework. From a practical perspective, we consider ECG data as image

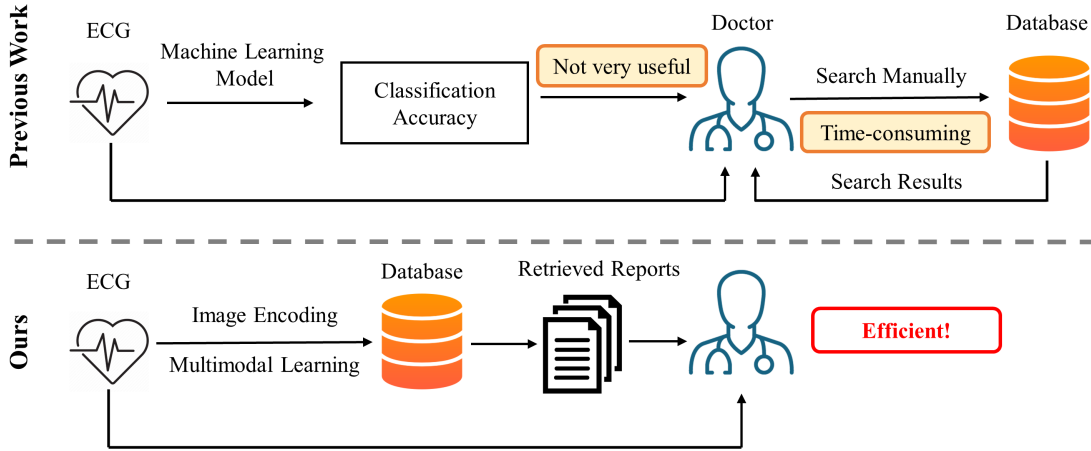


Figure 1: Comparison of our approach with previous works. In previous studies, machine learning models are only able to provide disease prediction accuracy, which may not be useful enough since the doctors still need to search the database to cross-check previous studies for accurate diagnosis. In contrast, our approach can retrieve the most relevant previous studies for the doctors, which can dramatically reduce doctors’ effort in manual search, which can lead to more efficient patient care and treatment.

input and use a set of featurization techniques. Our model learns to identify the similarity score between the two modalities so that the correspondence between an ECG image and its human language description can be automatically detected. Our contribution can be summarized as follows,

- In addition to traditional supervised learning classification tasks, we propose an approach to enhance ML-driven ECG automatic diagnosis by addressing the multimodal retrieval problem and learning to align the two modalities.
- We introduce a robust framework that offers clinicians a practical and efficient means to automatically search and identify similar ECG records for newly acquired ECG data.
- Capitalizing on the advancements in image-text alignment research, we emphasize treating ECG signals as images and present a variety of preprocessing techniques. This approach renders our method practical and easily adoptable, considering the extensive deployment of commercial ECG machines.

Generalizable Insights about Machine Learning in the Context of Healthcare

The burgeoning popularity of utilizing AI and ML algorithms for ECG interpretation and detecting cardiovascular disease can be attributed to their remarkable versatility and vast potential for addressing a diverse range of healthcare needs. These cutting-edge technologies hold significant promise for revolutionizing the field of cardiology by providing accurate

diagnoses, enhancing treatment outcomes, and improving patient care.

(A) However, most studies focus on extending off-the-shelf ML methods to ECG data, neglecting the **multimodality** in ECG information. ECG signals cannot simply be viewed as a classification problem because of the inherent correlation between different cardiovascular diseases. Therefore, clinicians provide language reports for each ECG trial. Our work aims to bridge the gap between different modalities within ECG datasets.

(B) Despite the robustness, fairness, and privacy advances in AI algorithms, the blackbox nature of deep learning models makes them unsuitable for deployment in critical real-world applications. To address this, our retrieval module can locate the most relevant ECG record and diagnostic in an existing database, enhancing the **credibility** of downstream AI-generated diagnostics.

(C) Additionally, healthcare information systems in underdeveloped regions may not support sophisticated ML diagnostic systems. Our method offers an **economical and accessible** approach to connect raw paper-printed ECG images to those stored and analyzed, allowing people in underdeveloped regions to utilize the information system and ML services built in developed environments.

2. Related Work

Multimodal Learning in Healthcare The computational field of machine learning has faced the multimodal nature of clinical expert decision-making. [Kline et al. \(2022\)](#) summarized the current studies in multimodal learning in healthcare applications and identified topics ripe for future research. [Amal et al. \(2022\)](#) reviewed multimodal data fusion and machine learning in cardiovascular medicine. For example, the detection of cardiac amyloidosis can benefit from fusing ECG signals and echocardiograms with convolution neural networks ([Goto et al., 2021](#)). The multimodal approach also helps as combining salient physiological signals and EHR data can effectively predict the onset of hemodynamic decompensation ([Hernandez et al., 2021](#)). However, our study is the first to investigate the multimodal properties between ECG and natural language data.

Encode Time Series Signals into Images Deep learning has been successfully applied to automate ECG diagnosis ([Han et al., 2020b](#)). These methods are usually based on raw ECG signal data and corresponding features ([Kiranyaz et al., 2015](#); [Zhu et al., 2022](#)). However, traditionally, ECG data is transformed into printed images with waveforms and interpreted by trained clinicians ([Sangha et al., 2022a](#)). To take advantage of the recent achievements in deep learning computer vision and provide more practical and accessible benefits for ECG interpretation, ML methods that treat ECG data as image features have been explored. An early approach combined either ECG images or signals ([Sangha et al., 2022a](#)) as inputs for cardiac disease diagnosis. Specifically, a convolutional neural network based on the EfficientNet architecture was built for ECG images. The idea of interpreting printed ECG papers has also been shown to be effective for diagnosing left ventricular (LV) systolic dysfunction ([Sangha et al., 2022b](#)). Additionally, digitizing printed ECG papers by scanning and processing raw printed images ([Wu et al., 2022](#)) is a critical task. Similarly, an automated ECG diagnostic pipeline using paper-ECG images can help provide accessible diagnosis services in underdeveloped regions where healthcare information systems are limited and only paper-printed ECGs are available.

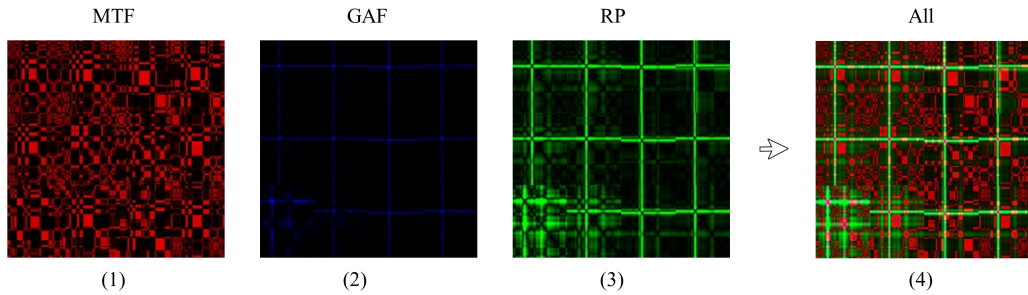


Figure 2: Examples of encoded ECG images by (1) MTF; (2) GAF; (3) RP; and (4) combine all three methods in three channels.

3. Methods

This application is relatively complex and may be challenging for some individuals to fully comprehend due to the use of technical language and advanced concepts related to ECG retrieval systems and their potential impact on clinical applications. Additionally, the statement assumes a certain level of knowledge and familiarity with the field of cardiology and the role of ECG data in diagnosing cardiac conditions, which may be a barrier for individuals who are less familiar with these topics. However, for those with a background in medicine or related fields, the statement provides a thorough and detailed analysis of the potential benefits of ECG retrieval systems in clinical settings.

A doctor’s diagnosis report can be instrumental in solving the potential complexity of the usefulness of ECG retrieval systems in clinical applications. By providing clear and concise descriptions of the benefits of such systems in diagnosing cardiac conditions, doctors can help break down complex technical language and concepts into more accessible terms for patients and other individuals who may be less familiar with these topics. For example, a doctor’s diagnosis report may explain how an ECG retrieval system can quickly and accurately identify abnormalities in heart function, which can lead to more timely and effective treatment for patients with cardiac conditions. Additionally, the report may describe how ECG data can be stored and analyzed using these systems, allowing doctors to easily access and review patient information to make more informed decisions about diagnosis and treatment.

3.1. Encode ECG Signals into Images

In our study, we employed three distinct encoding techniques to convert ECG time series signals into visual representations, namely Markov Transition Field (MTF), Gramian Angular Field (GAF), and Recurrence Plot (RP). A detailed overview of each method is provided in the subsequent sections.

3.1.1. MARKOV TRANSITION FIELD (MTF)

Markov Transition Field (MTF) is a method of transforming time series data, such as ECG signals, into visual representations. MTF works by calculating transition probabilities between adjacent data points in a time series, and then using these probabilities to generate

a matrix of color-coded pixels. Each pixel in the matrix represents a unique transition probability, with darker colors indicating higher probabilities and lighter colors indicating lower probabilities. This matrix can be thought of as an image that encapsulates the key features of the original time series, making it easier for researchers and clinicians to analyze and interpret ECG signals. The development of the Markov Transition Field (MTF) draws inspiration from prior research on the interrelationship between time series and complex networks (Campanharo et al., 2011; Zheng et al., 2014; Wang and Oates, 2014). In essence, the MTF methodology involves constructing a Markov matrix based on quantile bins, which are derived through the discretization of the time series data. The dynamic transition probability of the time series is then encoded into a quasi-Gramian matrix, facilitating further analysis and interpretation of the underlying complex system.

In order to preserve time-domain information, the proposed method leverages Markov transfer probability to represent the dynamics of a given time series X . Specifically, the Q quantile bins are identified, and each data point x_i is assigned to its corresponding bin $q_j (j \in [1, Q])$. The resulting weighted adjacency matrix W , constructed using a first-order Markov chain model along the time axis, reflects the transition probabilities among the quantile bins. The frequency with which a data point in quantile bin q_j is followed by a point in bin q_i determines the value of the corresponding entry $w_{i,j}$ in W . Although W represents the Markov transition matrix after normalization by $\sum_j w_{ij} = 1$, it is insensitive to the distribution of X and the temporal dependencies between time steps t_i , resulting in a loss of information. To address this issue, the Markov Transition Field (MTF) M is defined as follows:

$$\begin{bmatrix} w_{ij|x_1 \in q_i, x_1 \in q_j} & w_{ij|x_1 \in q_i, x_2 \in q_j} & \cdots & w_{ij|x_1 \in q_i, x_n \in q_j} \\ w_{ij|x_2 \in q_i, x_1 \in q_j} & w_{ij|x_2 \in q_i, x_2 \in q_j} & \cdots & w_{ij|x_2 \in q_i, x_n \in q_j} \\ \vdots & \vdots & \ddots & \vdots \\ w_{ij|x_n \in q_i, x_1 \in q_j} & w_{ij|x_n \in q_i, x_2 \in q_j} & \cdots & w_{ij|x_n \in q_i, x_n \in q_j} \end{bmatrix} \quad (1)$$

It involves building a $Q \times Q$ Markov transition matrix W by dividing the time series data into Q quantile bins, where q_i and $q_j (q \in [1, Q])$ represent the quantile bins that contain the data at time stamps i and j along the temporal axis. The MTF matrix M encodes the transition probabilities of the time series by spreading out the transition probability values from matrix W along the magnitude axis to M while taking into consideration the temporal positions. At each pixel M_{ij} , the probability of transitioning from the quantile at time step i to the quantile at time step j is assigned. In this way, the MTF matrix M captures the multi-span transition probabilities of the time series. The entry $M_{i,j||i-j|=k}$ in M represents the transition probability between points with a time interval of k , where $M_{i,j||j-i|=1}$ represents the transition process along the time axis with a skip step. The main diagonal M_{ii} in M is a special case when $k = 0$ and captures the probability of transitioning from each quantile to itself, i.e., the self-transition probability, at time step i .

3.1.2. GRAMIAN ANGULAR FIELD (GAF)

Gramian Angular Field (GAF) (Wang and Oates, 2014) is another method for transforming ECG time series signals into visual representations. GAF generates a matrix of cosine and sine values based on the pairwise differences between the original data points in the time

series. This matrix is then transformed into an image, where each pixel corresponds to a particular combination of cosine and sine values. Similar to MTF, the resulting image captures important features of the original ECG signal, such as patterns and trends, which can aid in the interpretation and analysis of the data. The advantage of GAF over MTF is that it preserves the phase information of the original time series, which can be important in some applications, such as detecting arrhythmias.

The Gramian Angular Field (GAF) (Wang and Oates, 2014) method represents time series data in a polar coordinate system instead of using the traditional Cartesian coordinates. In the Gramian matrix of GAF, each element corresponds to the cosine of the summation of angles. The rescaled time series \tilde{X} of n real-valued observations are transformed to fall within the range of $[-1, 1]$ or $[0, 1]$ using the formula:

$$\tilde{x}_{-1}^i = \frac{(x_i - \max(X) + (x_i - \min(X)))}{\max(X) - \min(X)} \quad (2)$$

$$\text{or } \tilde{x}_0^i = \frac{x_i - \min(X)}{\max(X) - \min(X)} \quad (3)$$

Then, by encoding the value as the angular cosine and the time stamp as the radius, we represent the rescaled time series \tilde{X} in polar coordinates as follows:

$$\phi = \arccos(\tilde{x}_i), \quad -1 \leq \tilde{x}_i \leq 1, \quad \tilde{x}_i \in \tilde{X}, \quad r = \frac{t_i}{N}, \quad t_i \in N \quad (4)$$

Here, t_i is the time stamp, and N is a constant factor that regulates the span of the polar coordinate system. This encoding technique is a novel way to visualize time series data, where the values transform among different angular positions on the spanning circles as time passes, resembling water rippling. The encoding map is bijective, and it preserves absolute temporal relations, unlike Cartesian coordinates. The angular cosine function is monotonic for $\phi \in [0, \pi]$, producing a unique result in the polar coordinate system with a one-to-one inverse map.

Rescaled data in different intervals have different angular bounds. $[0, 1]$ corresponds to the cosine function in $[0, \pi/2]$, while cosine values in the interval $[-1, 1]$ fall into the angular bounds $[0, \pi]$. They can provide different information granularity in the Gramian Angular Field for classification tasks, and the Gramian Angular Difference Field (GADF) of $[0, 1]$ rescaled data has an accurate inverse map. This property actually lays the foundation for imputing the missing value of time series by recovering the images.

We can utilize the angular perspective of the polar coordinate system to examine temporal correlations between different time intervals by calculating the trigonometric sum/difference between each point. Specifically, we can define the Gramian Summation Angular Field (GASF) and Gramian Difference Angular Field (GADF) as follows:

$$GASF = [\cos(\phi_i + \phi_j)] = \tilde{X}' \cdot \tilde{X} - \sqrt{I - \tilde{X}^2}' \cdot \sqrt{I - \tilde{X}^2} \quad (5)$$

$$GADF = [\sin(\phi_i - \phi_j)] = \sqrt{I - \tilde{X}^2}' \cdot \tilde{X} - \tilde{X}' \cdot \sqrt{I - \tilde{X}^2} \quad (6)$$

Here, I is the unit row vector $[1, 1, \dots, 1]$. After transforming the time series into the polar coordinate system, we treat each time step as a 1-D metric space. Defining the inner product as follows:

$$\langle x, y \rangle_1 = x \cdot y - \sqrt{1 - x^2} \cdot \sqrt{1 - y^2} \quad (7)$$

$$\langle x, y \rangle_2 = \sqrt{1 - x^2} \cdot y - x \cdot \sqrt{1 - y^2} \quad (8)$$

The two types of Gramian Angular Fields (GAFs) are actually quasi-Gramian matrices $[\langle \tilde{x}_1, \tilde{x}_1 \rangle]$.

The Gramian Angular Fields (GAFs) offer multiple benefits. First, they enable the retention of temporal relationships, as the position's movement from the top-left to the bottom-right corresponds to the increase in time. The GAFs incorporate temporal correlations since $G_{i,j||i-j|=k}$ symbolizes the relative correlation due to the superimposition/difference of directions concerning time interval k . The main diagonal $G_{i,i}$ is a special case for $k = 0$, containing the original angular/value information.

3.1.3. RECURRENCE PLOT (RP)

Recurrence Plot (RP) (Eckmann et al., 1987) is a non-linear time series analysis technique that can also be applied to transform ECG time series signals into visual representations. RP generates a square matrix that reflects the similarity between all pairs of data points in the time series. The matrix is constructed by measuring the distance between each pair of data points and comparing them to a predefined threshold value. If the distance between two points is below the threshold, the corresponding matrix element is set to 1, otherwise, it is set to 0. This results in a binary matrix that can be visualized as an image, where dark pixels represent recurrent patterns in the time series. RP has been shown to be effective in capturing complex patterns in ECG signals, such as P-waves and QRS complexes, which are important for the accurate diagnosis of cardiovascular diseases.

Given a time series (x_1, \dots, x_n) , we can extract trajectories from it as follows:

$$\mathbf{x}i = (x_i, x_{i+\tau}, \dots, x_{i+(m-1)\tau}), \quad \forall i \in 1, \dots, n - (m-1)\tau \quad (9)$$

Here, m denotes the dimension of the trajectories, and τ is the time delay. Once we have extracted the trajectories, we can create a recurrence plot, denoted by R , which is essentially the pairwise distance between the trajectories. Formally, we define $R_{i,j}$ as:

$$R_{i,j} = \Theta(\varepsilon - |\mathbf{x}_i - \mathbf{x}_j|), \quad \forall i, j \in 1, \dots, n - (m-1)\tau \quad (10)$$

Here, Θ is the Heaviside step function, and ε is the threshold. The recurrence plot helps us visualize the structure and patterns of the time series by preserving the temporal dependencies and revealing the relative correlations between the extracted trajectories.

3.2. Model Architecture

This section commences with an overview of the model architecture, followed by a detailed account of the training objectives. An elaborate illustration of the model architecture is presented in Figure 3, which includes a vision encoder responsible for processing visual information, a language encoder dedicated to understanding textual data, and a multimodal encoder that integrates information from both the vision and language encoders to form a robust representation.

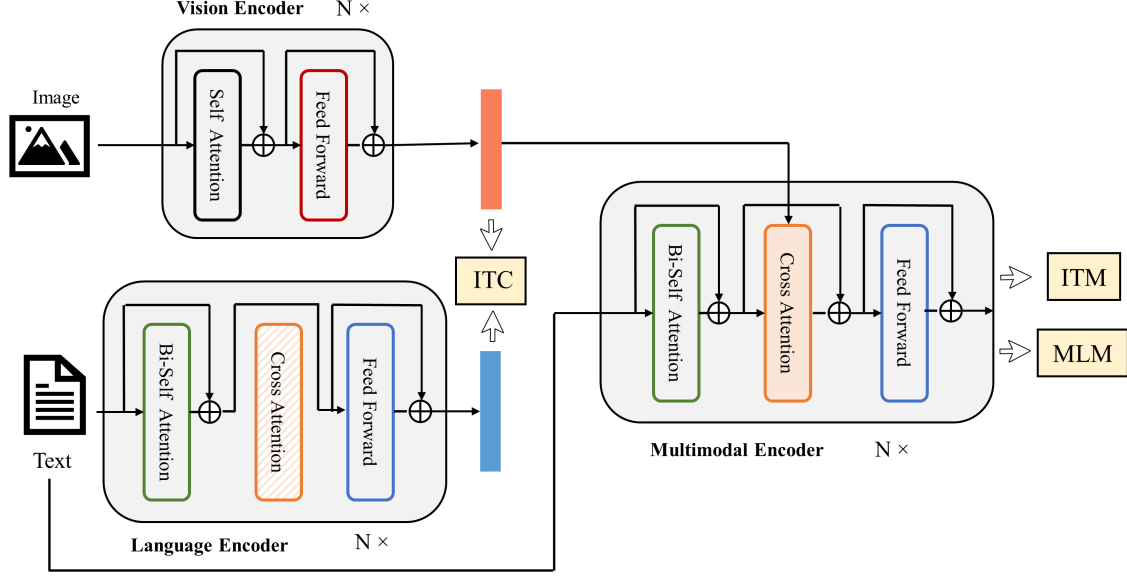


Figure 3: The overall architecture of our model. This architecture comprises a vision encoder responsible for processing visual data, a language encoder that focuses on comprehending textual information, and a multimodal encoder that combines the input from both the vision and language encoders to create a strong and comprehensive representation.

Vision Encoder Our current vision encoder architecture is based on a visual transformer (Dosovitskiy et al., 2021), which implements a patch-based processing approach that encodes an input image into a sequence of embeddings. This is achieved by dividing the image into patches and then performing a sequence of encoding operations on each patch. In addition, an extra [CLS] token is included to represent the global image feature. This approach has been shown to be more computation-friendly than using pre-trained object detectors for visual feature extraction (Chen et al., 2020c) and has been adopted by more recent methods such as ALBEF and ViLT (Li et al., 2021a; Kim et al., 2021b). Specifically, given an input image I , the ViT-based vision encoder generates a sequence of embeddings: $v_{\text{cls}}, v_1, \dots, v_N$. Here, v_{cls} represents the embedding of the [CLS] token, and the remaining v_i represents the patch embeddings. It is worth noting that this patch-based processing approach allows the vision encoder to capture fine-grained details of the input image, which can be important for downstream tasks that require a high level of visual understanding.

Language Encoder Our text encoder is based on the highly effective BERT architecture (Devlin et al., 2019b), which employs a [CLS] token appended to the beginning of the input text to provide a summary of the sentence. The encoder also utilizes a bi-directional self-attention mechanism to generate representations for each of the input tokens. This approach is highly effective for capturing the context and meaning of each token in the input text, enabling the model to better understand the overall meaning of the text. When processing an input text T , the text encoder generates a sequence of embed-

dings $\mathbf{w}_{\text{cls}}, \mathbf{w}_1, \dots, \mathbf{w}_N$, where \mathbf{w}_{cls} represents the embedding of the [CLS] token, and the remaining \mathbf{w}_i represent the embeddings of the individual input tokens. This sequence of embeddings is then passed to the multimodal encoder, where it is combined with the visual embeddings generated by the vision encoder.

Multimodal Encoder The multimodal encoder is a complex module that plays a critical role in enabling the model to learn the relationships between the visual and textual inputs. To achieve this, it incorporates an additional cross-attention (CA) layer that sits between the self-attention (SA) layer and the feed-forward network (FFN) for each transformer block of the text encoder. By doing so, the model can attend to both the textual and visual inputs and build better representations of the image-text pair. To create a multimodal representation of the image-text pair, the text input is modified by appending a task-specific [Encode] token at the end of the sequence, which is then fed into the multimodal encoder. The output embedding of this token is used as the final representation of the image-text pair. The embedding layers, CA layers, and FFN share similar functionality between encoding and decoding tasks, which means that they can be shared to improve training efficiency and benefit from multi-task learning. Additionally, the cross-attention layer introduces another set of attention weights to the model, which requires additional computation and increases the number of parameters to be learned. However, this additional complexity is necessary to enable the model to learn the relationships between the visual and textual inputs and to achieve state-of-the-art performance on various image-text tasks.

3.3. Loss Objectives

There are three objectives during learning, including Image-Text Contrastive (ITC) Loss, Image-Text Matching (ITM) Loss, and Mask Language Modeling (MLM) Loss.

Image-Text Contrastive Loss (ITC) The Image-Text Contrastive Loss (ITC) is a powerful objective function that activates the unimodal encoder and encourages the alignment of the visual transformer and the text transformer feature spaces by ensuring that similar image-text pairs have similar representations while dissimilar pairs have dissimilar ones. This objective has been shown to be highly effective in improving vision and language understanding in a range of applications, including image captioning, visual question answering, and multimodal retrieval (Radford et al., 2021b; Li et al., 2021a). To compute the ITC loss, we follow the approach proposed by Li et al. (2021a), which introduces a momentum encoder to generate features and creates soft labels from the momentum encoder to serve as training targets. The soft labels help account for the potential positive samples in the negative pairs and improve the quality of the learned representations. By optimizing the ITC loss, our model can better understand the relationships between images and their associated text, leading to improved performance on various vision and language tasks.

To achieve this, our model learns a similarity function represented by

$$s = g_v(\mathbf{v}_{\text{cls}})^\top g_w(\mathbf{w}_{\text{cls}}) \quad (11)$$

which aims to increase the similarity scores for matching image-text pairs. Here, g_v and g_w refer to linear transformations that convert the [CLS] embeddings into lower-dimensional, normalized (256-d) representations. Following the MoCo approach (He et al., 2020), we

use two queues to store the most recent M image-text representations obtained from the momentum unimodal encoders. The features obtained from the momentum encoders are normalized and denoted by $g'v(\mathbf{v}'_{\text{cls}})$ and $g'w(\mathbf{w}'_{\text{cls}})$. To calculate the similarity score between an image-text pair and a text-image pair, we define $s(I, T) = g_v(\mathbf{v}_{\text{cls}})^\top g'w(\mathbf{w}'_{\text{cls}})$ and $s(T, I) = g_w(\mathbf{w}_{\text{cls}})^\top g'v(\mathbf{v}'_{\text{cls}})$, respectively.

We use the softmax-normalized image-to-text and text-to-image similarity to calculate each image and text. This is represented by the equations below, where τ is a temperature parameter that can be learned:

$$p_m^{\text{i2t}}(I) = \frac{\exp(s(I, T_m)/\tau)}{\sum_{m=1}^M \exp(s(I, T_m)/\tau)}, \quad p_m^{\text{t2i}}(T) = \frac{\exp(s(T, I_m)/\tau)}{\sum_{m=1}^M \exp(s(T, I_m)/\tau)} \quad (12)$$

We represent the ground-truth one-hot similarity as $\mathbf{y}^{\text{i2t}}(I)$ and $\mathbf{y}^{\text{t2i}}(T)$, where negative pairs have a probability of 0, and the positive pair has a probability of 1. The image-text contrastive loss is defined as the cross-entropy H between \mathbf{p} and \mathbf{y} , which is shown in the following equation:

$$\mathcal{L}_{\text{itc}} = \frac{1}{2} \mathbb{E}(I, T) \sim D[H(\mathbf{y}^{\text{i2t}}(I), \mathbf{p}^{\text{i2t}}(I)) + H(\mathbf{y}^{\text{t2i}}(T), \mathbf{p}^{\text{t2i}}(T))] \quad (13)$$

Image-Text Matching Loss (ITM) The Image-Text Matching Loss (ITM) is responsible for activating the image-grounded text encoder, with the goal of learning a multimodal representation that captures the detailed alignment between visual and linguistic information. ITM is a binary classification task where the model predicts whether an image-text pair is positive (matched) or negative (unmatched) based on its multimodal feature. The ITM head, which is a linear layer, is used to make this prediction.

To obtain the joint representation of the image-text pair, we use the output embedding of the [CLS] token from the multimodal encoder, and then append a fully-connected (FC) layer followed by softmax to predict a two-class probability p^{itm} . The ITM loss is defined as:

$$\mathcal{L}_{\text{itm}} = \mathbb{E}(I, T) \sim DH(\mathbf{y}^{\text{itm}}, \mathbf{p}^{\text{itm}}(I, T)) \quad (14)$$

where \mathbf{y}^{itm} is a 2-dimensional one-hot vector representing the ground-truth label. To improve the selection of negative pairs, we employ a strategy called hard negative mining, as proposed by Li et al. (2021a). This strategy involves selecting negative pairs that have a higher contrastive similarity within a batch, as they are more informative and can improve the learning process.

Mask Language Modeling Loss (MLM) The Mask Language Modeling Loss (MLM) is used to predict masked words using both the image and contextual text. In this loss, we randomly mask out input tokens with a probability of 15% and replace them with the special token [MASK], with 10% random tokens, 10% unchanged, and 80% [MASK] replacements following the BERT approach. The predicted probability of a masked token is denoted by $\mathbf{p}^{\text{msk}}(I, \hat{T})$, where \hat{T} represents the masked text. The cross-entropy loss is used to minimize the difference between the predicted and ground-truth distributions, which is expressed as follows:

$$\mathcal{L}_{\text{mlm}} = \mathbb{E}(I, \hat{T}) \sim DH(\mathbf{y}^{\text{msk}}, \mathbf{p}^{\text{msk}}(I, \hat{T})) \quad (15)$$

Here, \mathbf{y}^{msk} represents a one-hot vocabulary distribution where the ground-truth token has a probability of 1.

4. Experiments

4.1. Dataset and Preprocessing

Our experiments were conducted using the PTB-XL dataset (Wagner et al., 2020), which comprises clinical 12-lead ECG signals that are 10 seconds in length. The dataset includes five different conditions: Normal ECG (NORM), Myocardial Infarction (MI), ST/T Change (STTC), Conduction Disturbance (CD), and Hypertrophy (HYP). The waveform files are stored in the WaveForm DataBase (WFDB) format and have a precision of 16 bits at a resolution of $1\mu\text{V}/\text{LSB}$, with a sampling frequency of 100Hz. The raw waveform data was annotated by up to two cardiologists who assigned one or more ECG statements to each record, resulting in a total of 71 different ECG statements that conform to the SCP-ECG standard. These statements cover diagnostic, form, and rhythm-related information. Additionally, the dataset contains extensive metadata on demographics, infarction characteristics, likelihoods for diagnostic ECG statements, as well as annotated signal properties.

To convert the time series data into a spectrum, we leveraged the WFDB library (Xie et al.) to read the raw data and performed Fast Fourier Transform (FFT). In order to eliminate noise, we implemented n-points window filtering, and to eliminate power frequency interference, which occurs at 50Hz, we employed notch processing with a quality factor of 30 (Qiu et al., 2022c).

4.2. Experimental Setting

The initialization of our visual encoder, text encoder, and multimodal encoder was carried out using the image encoder, text encoder, and image-grounded text encoder from Li et al. (2022), respectively. Specifically, the visual encoder was based on ViT (Dosovitskiy et al., 2020) pre-trained on ImageNet (He et al., 2015), while the other two encoders were initialized from BERT (Devlin et al., 2019a). All three encoders were trained on a dataset consisting of 14M images from COCO (Lin et al., 2014), Visual Genome (Krishna et al., 2016), Conceptual Captions (Sharma et al., 2018), Conceptual 12M (Changpinyo et al., 2021), and SBU captions (Ordonez et al., 2011), as described in Li et al. (2022).

Next, we fine-tuned the three encoders on our ECG image data using the AdamW optimizer (Loshchilov and Hutter, 2017) with a weight decay of 0.05. The learning rate was warmed-up to $3\text{e-}4$ (for ViT-B) / $2\text{e-}4$ (for ViT-L) and decayed linearly with a rate of 0.85. During fine-tuning, we randomly cropped images to a resolution of 384×384 . Our experiments were conducted on 2 NVIDIA A6000 GPUs and 2 NVIDIA A5000 GPUs. We evaluate our models using the recall at K (R@K) metric, where $K = 1, 5, 10$, and report the RSUM, which is the sum of the recall metrics at $K = 1, 5, 10$ for both video and text retrieval tasks.

4.3. Experimental Results and Discussions

Table 1 presents the results of our experiments comparing different image encoding methods. We conducted experiments in various settings to obtain a comprehensive understanding of the methods:

(1) The “Simple-plot” method serves as a straightforward baseline, where we plotted the ECG time series signals of 12 leads, selecting one ECG pause from each lead and putting

them in a 4×3 layout.

(2) Using each encoding method individually, we formulated three baseline approaches referred to as “MTF-only”, “GAF-only”, and “RP-only”.

(3) Two encoding methods were randomly selected from the three and concatenated in different image channels.

(4) Instead of encoding each lead independently, we concatenated the 12 leads of one ECG pause into a single vector, which we then visualized using all three encoding methods. This approach is referred to as “All-Concat”.

(5) Finally, we gridded all three encoding methods in three image channels under both zero-shot and fine-tune settings, referred to as “All-Grid (zero-shot)” and “All-Grid (fine-tune)”, respectively.

Table 1 presents the experimental findings, which indicate that for single encoding comparison, RP encoding significantly outperforms both MTF and GAF encoding techniques. Moreover, the combination of GAF and RP encoding demonstrates superior performance compared to the other two combinations. Remarkably, the “All-Grid (fine-tune)” method exhibits the best overall performance among all the baseline methods. A detailed analysis of the zero-shot and fine-tuning results shows that fine-tuning has a considerable impact on improving the performance of the models.

The “All-Grid (fine-tune)” method utilizes a fine-tuning approach to improve the performance of the models by iteratively adjusting the parameters of the network. This method achieves the best overall performance by effectively leveraging the available data. The analysis of the zero-shot and fine-tuning results indicates that fine-tuning significantly enhances the performance of the models, highlighting the importance of optimizing the network parameters to improve the accuracy of the predictions.

Table 1: Experimental results.

Method	Report Retrieval			Image Retrieval			RSUM
	R@1	R@5	R@10	R@1	R@5	R@10	
Simple-plot	5.51	17.16	25.64	4.98	17.08	26.05	96.42
MTF-only	1.42	5.67	10.72	1.97	6.07	10.80	36.65
GAF-only	2.69	10.53	17.04	3.22	11.01	17.60	62.09
RP-only	5.27	16.84	25.68	5.63	17.20	26.44	97.06
MTF+GAF	4.02	14.03	21.91	4.10	14.42	21.91	80.39
GAF+RP	6.30	21.04	30.36	6.93	20.69	30.65	115.97
PR+MTF	5.12	17.26	25.84	4.96	17.10	26.56	96.84
All-Concat	1.58	7.25	12.77	1.73	7.33	13.71	4.37
All-Grid (zero-shot)	0.21	1.06	1.91	0.43	1.06	1.91	6.58
All-Grid (fine-tune)	7.88	24.51	34.04	8.27	23.96	34.91	133.57

4.4. Ablation Study

In any modeling exercise, a vast array of parameters and settings can be adjusted to optimize performance. However, it is not always clear which of these factors has the most significant

impact on the final output. In order to gain a better understanding of the inner workings of our model and the effect that each individual parameter has on its performance, we conducted a series of ablation studies.

To gain insight into the impact of batch size on the training and testing of our model, we conducted an ablation study. In this study, we systematically varied the training and testing batch sizes, and the results are presented in Table 2. Surprisingly, we found that a smaller training batch size led to better performance. This observation may seem counterintuitive, as larger batch sizes are typically favored in deep learning to accelerate training. However, our results suggest that a smaller training batch size may help the model converge more quickly and reduce overfitting. In addition, we observed that a smaller testing batch size also contributed to improved performance, when the training batch size was kept the same. This finding highlights the importance of matching the testing batch size to the training batch size, to ensure that the model is evaluated on a representative sample of data. By carefully selecting the appropriate training and testing batch sizes, we can optimize our model and achieve better results.

Table 2: Ablation study on learning batch.

Batch	Report Retrieval			Image Retrieval			RSUM
	R@1	R@5	R@10	R@1	R@5	R@10	
Training 8 + Testing 32	7.88	24.51	34.04	8.27	23.96	34.91	133.57
Training 16 + Testing 32	7.88	22.54	32.23	7.32	21.91	33.41	125.29
Training 32 + Testing 32	7.01	20.88	32.23	6.78	21.04	32.47	120.41

In addition, we conducted an ablation study on the selection of the visual encoder. There are two choices of visual encoder selection: ViT-base and ViT-large. ViT-base has 12 transformer layers, about 85 million parameters, and is trained on images resized to 224x224 pixels. It is a relatively smaller model and is suitable for smaller datasets or where memory or computational resources are limited. ViT-large has 24 transformer layers, about 307 million parameters, and is trained on images resized to 384x384 pixels. It is a more complex and larger model, which typically results in better performance on large-scale datasets.

The results of the ablation study are summarized in Table 3. Notably, we observed that for both the All-Grid and All-Concat settings, ViT-base outperformed ViT-large in terms of classification accuracy. These results are surprising, as ViT-large has more parameters and has been shown to perform better than ViT-base on pretraining tasks. However, we posit that the reason for this discrepancy lies in the size of the ECG image dataset. Specifically, since the dataset is relatively small, the fine-tuned embeddings of the ViT-base can more quickly adapt to the unique features of ECG images. In contrast, ViT-large contains more parameters and may require a larger dataset for effective fine-tuning. These findings have important implications for the use of ViT in medical image analysis. While ViT has shown great promise in a variety of visual recognition tasks, it is important to carefully consider its performance when applied to medical imaging datasets. Our results suggest that ViT-base may be a better choice for small medical imaging datasets, while ViT-large may be more effective for larger datasets. Additionally, our study highlights the importance of conducting

careful evaluations of visual encoders in the medical imaging domain to ensure that they perform well on the specific imaging modality in question.

Table 3: Ablation study on vision encoder.

Vision Encoder	Report Retrieval			Image Retrieval			RSUM
	R@1	R@5	R@10	R@1	R@5	R@10	
All-concat (ViT-base)	2.52	8.91	13.79	2.52	7.25	12.77	47.76
All-concat (ViT-large)	1.58	7.25	12.77	1.73	7.33	13.71	44.37
All-Grid (ViT-base)	7.88	24.51	34.04	8.27	23.96	34.91	133.57
All-Grid (ViT-large)	3.47	12.32	21.43	4.73	14.26	22.14	78.35

5. Discussion

Drawing upon the experimental findings presented in the preceding section, it has come to our attention that the transformation of ECG time series signals into images presents a highly promising approach. Additionally, the integration of cutting-edge vision-language learning advancements can provide further benefits to the encoded images. Our proposed model suggests that joint learning of the encoded ECG images and doctor’s reports can lead to the acquisition of superior representations. These acquired representations have the potential to be advantageous in downstream clinical applications, such as the retrieval of the most pertinent previous diagnosis reports from a database, enabling the provision of robust and efficient support and reference for doctors. Consequently, this can result in significantly improved patient treatment outcomes. Given the high stakes involved in healthcare, improving patient treatment and care remains a crucial imperative. The integration of the proposed model in clinical applications has the potential to revolutionize the landscape of healthcare and significantly impact patient care outcomes. As such, we believe that our proposed model can be very useful and practical in the field of clinical applications, with significant benefits for patients, doctors, and the wider healthcare ecosystem.

Limitations While our study has shed light on the potential of using MTF, GAF, and RP methods to analyze ECG data, it is important to note that there may be other encoding techniques that could yield good results. Additionally, the size of the dataset used in this study may not be sufficiently large to account for the full variability and complexity of ECG signals. Moreover, the accuracy of the doctor’s report, which was used in multimodal learning, could be a potential limitation as it is subject to inter-observer variability and could affect the quality of the learned representations. Furthermore, factors such as patient demographics, medical history, and comorbidities were not taken into account, which could be investigated in future work for the generalizability of our findings. Therefore, further studies using larger and more diverse datasets, incorporating a wider range of analysis techniques and accounting for various confounding factors, are necessary to fully explore the potential of our direction.

References

- Demilade A. Adedinsewo, Habeeba Siddiqui, Patrick W. Johnson, Erika J Douglass, Michal Cohen-Shelly, Zachi I. Attia, Paul A. Friedman, Peter A. Noseworthy, and Rickey E. Carter. Digitizing paper based ecg files to foster deep learning based analysis of existing clinical datasets: An exploratory analysis. *Intelligence-Based Medicine*, 2022.
- Jean-Baptiste Alayrac, Jeff Donahue, Pauline Luc, Antoine Miech, Iain Barr, Yana Hasson, Karel Lenc, Arthur Mensch, Katie Millican, Malcolm Reynolds, Roman Ring, Eliza Rutherford, Serkan Cabi, Tengda Han, Zhitao Gong, Sina Samangooei, Marianne Monteiro, Jacob Menick, Sebastian Borgeaud, Andy Brock, Aida Nematzadeh, Sahand Sharifzadeh, Mikolaj Binkowski, Ricardo Barreira, Oriol Vinyals, Andrew Zisserman, and Karen Simonyan. Flamingo: a visual language model for few-shot learning. *ArXiv*, abs/2204.14198, 2022.
- Miquel Alfaras, Miguel C. Soriano, and Silvia Ortín. A fast machine learning model for ecg-based heartbeat classification and arrhythmia detection. *Frontiers in Physics*, 2019.
- Saeed Amal, Lida Safarnejad, Jesutofunmi A. Omiye, Ilies Ghanzouri, John H Cabot, and Elsie Gyang Ross. Use of multi-modal data and machine learning to improve cardiovascular disease care. *Frontiers in Cardiovascular Medicine*, 9, 2022.
- Zachi I Attia, Suraj Kapa, Francisco Lopez-Jimenez, Paul M McKie, Dorothy J Ladewig, Gaurav Satam, Patricia A Pellikka, Maurice Enriquez-Sarano, Peter A Noseworthy, Thomas M Munger, et al. Screening for cardiac contractile dysfunction using an artificial intelligence-enabled electrocardiogram. *Nature medicine*, 25(1):70–74, 2019a.
- Zachi I Attia, Peter A Noseworthy, Francisco Lopez-Jimenez, Samuel J Asirvatham, Abhishek J Deshmukh, Bernard J Gersh, Rickey E Carter, Xiaoxi Yao, Alejandro A Rabinstein, Brad J Erickson, et al. An artificial intelligence-enabled ecg algorithm for the identification of patients with atrial fibrillation during sinus rhythm: a retrospective analysis of outcome prediction. *The Lancet*, 394(10201):861–867, 2019b.
- Yehualashet Megersa Ayano, Friedhelm Schwenker, Bisrat Derebssa Dufera, and Taye Girma Debelee. Interpretable machine learning techniques in ecg-based heart disease classification: A systematic review. *Diagnostics*, 13, 2022.
- Saira Aziz, Sajid Ahmed, and Mohamed-Slim Alouini. Ecg-based machine-learning algorithms for heartbeat classification. *Scientific Reports*, 11, 2021.
- Lan-Qing Bao, Jieli Qiu, Hao Tang, Wei-Long Zheng, and Bao-Liang Lu. Investigating sex differences in classification of five emotions from eeg and eye movement signals. *2019 41st Annual International Conference of the IEEE Engineering in Medicine and Biology Society (EMBC)*, pages 6746–6749, 2019.
- Silvio Barra, Salvatore M. Carta, Andrea Corrigan, Alessandro Sebastian Podda, and Diego Reforgiato Recupero. Deep learning and time series-to-image encoding for financial forecasting. *IEEE/CAA Journal of Automatica Sinica*, 7:683–692, 2020.

- Behnam Behinaein, Anubha Bhatti, Dirk Rodenburg, Paul C. Hungler, and Ali Etemad. A transformer architecture for stress detection from ecg. *2021 International Symposium on Wearable Computers*, 2021.
- Jianwei Bi, Hui Li, and Zhiyuan Fan. Tourism demand forecasting with time series imaging: A deep learning model. *Annals of Tourism Research*, 90:103255, 2021.
- Qiong Cai, Hao Wang, Zhenmin Li, and Xinyu Liu. A survey on multimodal data-driven smart healthcare systems: Approaches and applications. *IEEE Access*, 7:133583–133599, 2019.
- Andriana S. L. O. Campanharo, M. Irmak Sirer, R. Dean Malmgren, Fernando M. Ramos, and Luis A. Nunes Amaral. Duality between time series and networks. In *PloS one*, 2011.
- Soravit Changpinyo, Piyush Kumar Sharma, Nan Ding, and Radu Soricut. Conceptual 12m: Pushing web-scale image-text pre-training to recognize long-tail visual concepts. *2021 IEEE/CVF Conference on Computer Vision and Pattern Recognition (CVPR)*, pages 3557–3567, 2021.
- Chao Che, Peiliang Zhang, Min Zhu, Yue Qu, and Bo Jin. Constrained transformer network for ecg signal processing and arrhythmia classification. *BMC Medical Informatics and Decision Making*, 21, 2021.
- Huangxun Chen, Chenyu Huang, Qianyi Huang, Qian Zhang, and Wei Wang. Ecgadv: Generating adversarial electrocardiogram to misguide arrhythmia classification system. In *Proceedings of the AAAI Conference on Artificial Intelligence*, volume 34, pages 3446–3453, 2020a.
- Yen-Chun Chen, Linjie Li, Licheng Yu, Ahmed El Kholy, Faisal Ahmed, Zhe Gan, Yu Cheng, and Jingjing Liu. Uniter: Universal image-text representation learning. In *ECCV*, 2020b.
- Yen-Chun Chen, Linjie Li, Licheng Yu, Ahmed El Kholy, Faisal Ahmed, Zhe Gan, Yu Cheng, and Jingjing Liu. UNITER: universal image-text representation learning. In *ECCV*, volume 12375, pages 104–120, 2020c.
- Jacob Devlin, Ming-Wei Chang, Kenton Lee, and Kristina Toutanova. Bert: Pre-training of deep bidirectional transformers for language understanding. *ArXiv*, abs/1810.04805, 2019a.
- Jacob Devlin, Ming-Wei Chang, Kenton Lee, and Kristina Toutanova. BERT: pre-training of deep bidirectional transformers for language understanding. In Jill Burstein, Christy Doran, and Tamar Solorio, editors, *NAACL*, pages 4171–4186, 2019b.
- Alexey Dosovitskiy, Lucas Beyer, Alexander Kolesnikov, Dirk Weissenborn, Xiaohua Zhai, Thomas Unterthiner, Mostafa Dehghani, Matthias Minderer, Georg Heigold, Sylvain Gelly, Jakob Uszkoreit, and Neil Houlsby. An image is worth 16x16 words: Transformers for image recognition at scale. *ArXiv*, abs/2010.11929, 2020.

- Alexey Dosovitskiy, Lucas Beyer, Alexander Kolesnikov, Dirk Weissenborn, Xiaohua Zhai, Thomas Unterthiner, Mostafa Dehghani, Matthias Minderer, Georg Heigold, Sylvain Gelly, Jakob Uszkoreit, and Neil Houlsby. An image is worth 16x16 words: Transformers for image recognition at scale. In *ICLR*, 2021.
- Zi-Yi Dou, Yichong Xu, Zhe Gan, Jianfeng Wang, Shuohang Wang, Lijuan Wang, Chengguang Zhu, Nanyun Peng, Zicheng Liu, and Michael Zeng. An empirical study of training end-to-end vision-and-language transformers. *ArXiv*, abs/2111.02387, 2021.
- Jean-Pierre Eckmann, Sylvie Oliffson Kamphorst, and David Ruelle. Recurrence plots of dynamical systems. *EPL*, 4:973–977, 1987.
- Zhaoji Fu, Shenda Hong, Rui Zhang, and Shaofu Du. Artificial-intelligence-enhanced mobile system for cardiovascular health management. *Sensors*, 21(3):773, 2021.
- Zhe Gan, Yen-Chun Chen, Linjie Li, Chen Zhu, Yu Cheng, and Jingjing Liu. Large-scale adversarial training for vision-and-language representation learning. *ArXiv*, abs/2006.06195, 2020.
- Gabriel Rodriguez Garcia, Gabriel Michau, Mélanie Ducoffe, Jayant Sen Gupta, and Olga Fink. Temporal signals to images: Monitoring the condition of industrial assets with deep learning image processing algorithms. *Proceedings of the Institution of Mechanical Engineers, Part O: Journal of Risk and Reliability*, 236:617 – 627, 2020.
- Muhammad Ghulam, Fatima Alshehri, Fakhri Karray, Abdulmotaleb El Saddik, Mansour Alsulaiman, and Tiago H. Falk. A comprehensive survey on multimodal medical signals fusion for smart healthcare systems. *Inf. Fusion*, 76:355–375, 2021.
- John R. Giudicessi, Matthew Schram, J. Martijn Bos, Conner Galloway, Jacqueline Baras Shreibati, Patrick W. Johnson, Rickey E. Carter, Levi W Disrud, Robert B Kleiman, Zachi I. Attia, Peter A. Noseworthy, Paul A. Friedman, David E. Albert, and Michael J. Ackerman. Artificial intelligence-enabled assessment of the heart rate corrected qt interval using a mobile electrocardiogram device. *Circulation*, 2021.
- Bryan Gopal, Ryan Han, Gautham Raghupathi, Andrew Ng, Geoff Tison, and Pranav Rajpurkar. 3kg: contrastive learning of 12-lead electrocardiograms using physiologically-inspired augmentations. In *Machine Learning for Health*, pages 156–167. PMLR, 2021.
- Shinichi Goto, Keitaro Mahara, Lauren Beussink-Nelson, Hidehiko Ikura, Yoshinori Katsumata, Jin Endo, Hanna K Gaggin, Sanjiv J Shah, Yuji Itabashi, Calum A MacRae, et al. Artificial intelligence-enabled fully automated detection of cardiac amyloidosis using electrocardiograms and echocardiograms. *Nature communications*, 12(1):2726, 2021.
- Maya E Guglin and Deepak Thatai. Common errors in computer electrocardiogram interpretation. *International journal of cardiology*, 106(2):232–237, 2006.
- Xintian Han, Yuxuan Hu, Luca Foschini, Larry Chinitz, Lior Jankelson, and Rajesh Ranganath. Deep learning models for electrocardiograms are susceptible to adversarial attack. *Nature medicine*, 26(3):360–363, 2020a.

- Xintian Han, Yuxuan Hu, Luca Foschini, Larry Chinitz, Lior Jankelson, and Rajesh Ranganath. Deep learning models for electrocardiograms are susceptible to adversarial attack. *Nature medicine*, 26(3):360–363, 2020b.
- Awni Y Hannun, Pranav Rajpurkar, Masoumeh Haghpanahi, Geoffrey H Tison, Codie Bourn, Mintu P Turakhia, and Andrew Y Ng. Cardiologist-level arrhythmia detection and classification in ambulatory electrocardiograms using a deep neural network. *Nature medicine*, 25(1):65–69, 2019.
- Nima Hatami, Yann Gavet, and Johan Debayle. Classification of time-series images using deep convolutional neural networks. In *International Conference on Machine Vision*, 2017.
- Kaiming He, X. Zhang, Shaoqing Ren, and Jian Sun. Delving deep into rectifiers: Surpassing human-level performance on imagenet classification. *2015 IEEE International Conference on Computer Vision (ICCV)*, pages 1026–1034, 2015.
- Kaiming He, Haoqi Fan, Yuxin Wu, Saining Xie, and Ross Girshick. Momentum contrast for unsupervised visual representation learning. In *CVPR*, 2020.
- Larry Hernandez et al. Multimodal tensor-based method for integrative and continuous patient monitoring during postoperative cardiac care. *Artificial Intelligence in Medicine*, 113:102032, 2021.
- Shenda Hong, Zhaoji Fu, Rongbo Zhou, Jie Yu, Yongkui Li, Kai Wang, and Guanlin Cheng. Cardiolearn: a cloud deep learning service for cardiac disease detection from electrocardiogram. In *Companion Proceedings of the Web Conference 2020*, pages 148–152, 2020.
- Khondker Fariha Hossain, Sharif Amit Kamran, Alireza Tavakkoli, Lei Pan, Xingjun Ma, Sutharshan Rajasegarar, and Chandan Karmaker. Ecg-adv-gan: Detecting ecg adversarial examples with conditional generative adversarial networks. In *2021 20th IEEE International Conference on Machine Learning and Applications (ICMLA)*, pages 50–56. IEEE, 2021.
- Isaak Kavasidis, Simone Palazzo, Concetto Spampinato, Daniela Giordano, and Mubarak Shah. Brain2image: Converting brain signals into images. *Proceedings of the 25th ACM international conference on Multimedia*, 2017.
- Shaan Khurshid, Samuel N. Friedman, Christopher Reeder, Paolo Di Achille, Nathaniel Diamant, Pulkit Singh, Lia X. Harrington, Xin Wang, Mostafa A Al-alusi, Gopal Sarma, Andrea S. Foulkes, Patrick T. Ellinor, Christopher D. Anderson, Jennifer E. Ho, Anthony A. Philippakis, Puneet Batra, and Steven A. Lubitz. Ecg-based deep learning and clinical risk factors to predict atrial fibrillation. *Circulation*, 145:122 – 133, 2021.
- Sungsoo Kim, Sohee Kwon, Mia K. Markey, Alan Conrad Bovik, Sung Hwi Hong, Junyong Kim, Hye Jin Hwang, Boyoung Joung, Hui Nam Pak, Moon-Hyeong Lee, and Junbeom Park. Machine learning based potentiating impacts of 12-lead ecg for classifying paroxysmal versus non-paroxysmal atrial fibrillation. *International Journal of Arrhythmia*, 23: 1–9, 2022.

- Wonjae Kim, Bokyung Son, and Ildoo Kim. Vilt: Vision-and-language transformer without convolution or region supervision. In *ICML*, 2021a.
- Wonjae Kim, Bokyung Son, and Ildoo Kim. Vilt: Vision-and-language transformer without convolution or region supervision. *arXiv preprint arXiv:2102.03334*, 2021b.
- Serkan Kiranyaz, Turker Ince, Ridha Hamila, and M. Gabbouj. Convolutional neural networks for patient-specific ecg classification. *2015 37th Annual International Conference of the IEEE Engineering in Medicine and Biology Society (EMBC)*, pages 2608–2611, 2015.
- Adrienne S. Kline, Hanyin Wang, Yikuan Li, Saya Dennis, Meghan R. Hutch, Zhenxing Xu, Fei Wang, Feixiong Cheng, and Yuan Luo. Multimodal machine learning in precision health: A scoping review. *NPJ Digital Medicine*, 5, 2022.
- Ranjay Krishna, Yuke Zhu, Oliver Groth, Justin Johnson, Kenji Hata, Joshua Kravitz, Stephanie Chen, Yannis Kalantidis, Li-Jia Li, David A. Shamma, Michael S. Bernstein, and Li Fei-Fei. Visual genome: Connecting language and vision using crowdsourced dense image annotations. *International Journal of Computer Vision*, 123:32–73, 2016.
- Santosh Kumar, Mithilesh Kumar Chaube, Saeed Hamood Alsamhi, Sachin Kumar Gupta, Mohsen Guizani, Raffaele Gravina, and Giancarlo Fortino. A novel multimodal fusion framework for early diagnosis and accurate classification of covid-19 patients using x-ray images and speech signal processing techniques. *Computer Methods and Programs in Biomedicine*, 226:107109 – 107109, 2022.
- Junnan Li, Ramprasaath R. Selvaraju, Akhilesh Deepak Gotmare, Shafiq Joty, Caiming Xiong, and Steven Hoi. Align before fuse: Vision and language representation learning with momentum distillation. In *NeurIPS*, 2021a.
- Junnan Li, Ramprasaath R. Selvaraju, Akhilesh Deepak Gotmare, Shafiq R. Joty, Caiming Xiong, and Steven C. H. Hoi. Align before fuse: Vision and language representation learning with momentum distillation. In *NeurIPS*, 2021b.
- Junnan Li, Dongxu Li, Caiming Xiong, and Steven C. H. Hoi. Blip: Bootstrapping language-image pre-training for unified vision-language understanding and generation. In *International Conference on Machine Learning*, 2022.
- Xiujun Li, Xi Yin, Chunyuan Li, Xiaowei Hu, Pengchuan Zhang, Lei Zhang, Lijuan Wang, Houdong Hu, Li Dong, Furu Wei, Yejin Choi, and Jianfeng Gao. Oscar: Object-semantics aligned pre-training for vision-language tasks. In *ECCV*, 2020.
- Tsung-Yi Lin, Michael Maire, Serge J. Belongie, James Hays, Pietro Perona, Deva Ramanan, Piotr Dollár, and C. Lawrence Zitnick. Microsoft coco: Common objects in context. In *European Conference on Computer Vision*, 2014.
- Wei Liu, Jie-Lin Qiu, Wei-Long Zheng, and Bao-Liang Lu. Multimodal emotion recognition using deep canonical correlation analysis. *ArXiv*, abs/1908.05349, 2019.

- Wei Liu, Jieliu Qiu, Wei-Long Zheng, and Bao-Liang Lu. Comparing recognition performance and robustness of multimodal deep learning models for multimodal emotion recognition. *IEEE Transactions on Cognitive and Developmental Systems*, 14:715–729, 2021.
- Ilya Loshchilov and Frank Hutter. Decoupled weight decay regularization. In *International Conference on Learning Representations*, 2017.
- Giovanna Martínez-Arellano, Germán Terrazas, and Svetan M. Ratchev. Tool wear classification using time series imaging and deep learning. *The International Journal of Advanced Manufacturing Technology*, 104:3647 – 3662, 2019.
- Siddhartha Mishra, Gaurav Khatwani, Rupali Patil, Darshan Sapariya, Vruddhi Shah, Darshna Parmar, Sharath Dinesh, Prathamesh Daphal, and Ninad Dileep Mehendale. Ecg paper record digitization and diagnosis using deep learning. *Journal of Medical and Biological Engineering*, 41:422 – 432, 2020.
- Annamalai Natarajan, Yale Chang, Sara Mariani, Asif Rahman, Gregory Boverman, Shruti Gopal Vij, and Jonathan Rubin. A wide and deep transformer neural network for 12-lead ecg classification. *2020 Computing in Cardiology*, pages 1–4, 2020.
- Naoki Nonaka and Jun Seita. Electrocardiogram classification by modified efficientnet with data augmentation. In *2020 Computing in Cardiology*, pages 1–4. IEEE, 2020.
- Naoki Nonaka and Jun Seita. In-depth benchmarking of deep neural network architectures for ecg diagnosis. In *Proceedings of the 6th Machine Learning for Healthcare Conference*, Proceedings of Machine Learning Research, pages 414–439. PMLR, 2021.
- Janet E Olson, Euijung Ryu, Kiley J Johnson, Barbara A Koenig, Karen J Maschke, Jody A Morrisette, Mark Liebow, Paul Y Takahashi, Zachary S Fredericksen, Ruchi G Sharma, et al. The mayo clinic biobank: a building block for individualized medicine. In *Mayo Clinic Proceedings*, volume 88, pages 952–962. Elsevier, 2013.
- Vicente Ordonez, Girish Kulkarni, and Tamara L. Berg. Im2text: Describing images using 1 million captioned photographs. In *NIPS*, 2011.
- Xiangdong Pei, Ke Zuo, Yuan Li, and Zhengbin Pang. A review of the application of multimodal deep learning in medicine: Bibliometrics and future directions. *International Journal of Computational Intelligence Systems*, 16, 2023.
- Abdolrahman Peimankar and Sadasivan K. Puthusserypady. Dens-ecg: A deep learning approach for ecg signal delineation. *ArXiv*, abs/2005.08689, 2020.
- Zhen Qin, Yibo Zhang, Shuyu Meng, Zhiguang Qin, and Kim-Kwang Raymond Choo. Imaging and fusing time series for wearable sensor-based human activity recognition. *Inf. Fusion*, 53:80–87, 2020.
- Jieliu Qiu and Wei-Ye Zhao. Data encoding visualization based cognitive emotion recognition with ac-gan applied for denoising. *2018 IEEE 17th International Conference on Cognitive Informatics & Cognitive Computing (ICCI*CC)*, pages 222–227, 2018.

- Jielin Qiu, Xiaoyan Li, and Kai Hu. Correlated attention networks for multimodal emotion recognition. *2018 IEEE International Conference on Bioinformatics and Biomedicine (BIBM)*, pages 2656–2660, 2018a.
- Jielin Qiu, W. Liu, and Bao-Liang Lu. Multi-view emotion recognition using deep canonical correlation analysis. In *International Conference on Neural Information Processing*, 2018b.
- Jielin Qiu, Xin-Yi Qiu, and Kai Hu. Emotion recognition based on gramian encoding visualization. In *BI*, 2018c.
- Jielin Qiu, Jiacheng Zhu, Michael Rosenberg, Emerson Liu, and D. Zhao. Optimal transport based data augmentation for heart disease diagnosis and prediction. *ArXiv*, abs/2202.00567, 2022a.
- Jielin Qiu, Jiacheng Zhu, Mengdi Xu, Franck Dernoncourt, Trung Bui, Zhaowen Wang, Bo Li, Ding Zhao, and Hailin Jin. Semantics-consistent cross-domain summarization via optimal transport alignment. *ArXiv*, abs/2210.04722, 2022b.
- Jielin Qiu, Jiacheng Zhu, Mengdi Xu, Peide Huang, Michael Rosenberg, Douglas Weber, Emerson Liu, and Ding Zhao. Cardiac disease diagnosis on imbalanced electrocardiography data through optimal transport augmentation. 2022c.
- Jielin Qiu, Yi Zhu, Xingjian Shi, F. Wenzel, Zhiqiang Tang, D. Zhao, Bo Li, and Mu Li. Are multimodal models robust to image and text perturbations? *ArXiv*, abs/2212.08044, 2022d.
- Jielin Qiu, William Han, Jiacheng Zhu, Mengdi Xu, Michael Rosenberg, Emerson Liu, Douglas Weber, and Ding Zhao. Transfer knowledge from natural language to electrocardiography: Can we detect cardiovascular disease through language models? *ArXiv*, abs/2301.09017, 2023.
- Alec Radford, Jong Wook Kim, Chris Hallacy, Aditya Ramesh, Gabriel Goh, Sandhini Agarwal, Girish Sastry, Amanda Askell, Pamela Mishkin, Jack Clark, Gretchen Krueger, and Ilya Sutskever. Learning transferable visual models from natural language supervision. In *ICML*, 2021a.
- Alec Radford, Jong Wook Kim, Chris Hallacy, Aditya Ramesh, Gabriel Goh, Sandhini Agarwal, Girish Sastry, Amanda Askell, Pamela Mishkin, Jack Clark, et al. Learning transferable visual models from natural language supervision. *arXiv preprint arXiv:2103.00020*, 2021b.
- Aniruddh Raghu, Divya Shanmugam, Eugene Pomerantsev, John Gutttag, and Collin M Stultz. Data augmentation for electrocardiograms. In *Proceedings of the Conference on Health, Inference, and Learning*, Proceedings of Machine Learning Research, pages 282–310. PMLR, 2022.
- Sushravya Raghunath et al. Deep neural networks can predict new-onset atrial fibrillation from the 12-lead ecg and help identify those at risk of atrial fibrillation-related stroke. *Circulation*, 143:1287 – 1298, 2021.

- Aditya Ramesh, Prafulla Dhariwal, Alex Nichol, Casey Chu, and Mark Chen. Hierarchical text-conditional image generation with clip latents. *ArXiv*, abs/2204.06125, 2022.
- Unais Sait, Gokul Lal K.V., Sanjana Shivakumar, Tarun Kumar, Rahul Bhaumik, Sunny Prakash Prajapati, Kriti Bhalla, and Anaghaa Chakrapani. A deep-learning based multimodal system for covid-19 diagnosis using breathing sounds and chest x-ray images. *Applied Soft Computing*, 109:107522 – 107522, 2021.
- Veer Sangha, Bobak J Mortazavi, Adrian D Haimovich, Antônio H Ribeiro, Cynthia A Brandt, Daniel L Jacoby, Wade L Schulz, Harlan M Krumholz, Antonio Luiz P Ribeiro, and Rohan Khera. Automated multilabel diagnosis on electrocardiographic images and signals. *Nature communications*, 13(1):1583, 2022a.
- Veer Sangha, Arash A Nargesi, Lovedeep S Dhingra, Akshay Khunte, Bobak J Mortazavi, Antônio H Ribeiro, Evgeniya Banina, Oluwaseun Adeola, Nadish Garg, Cynthia A Brandt, et al. Detection of left ventricular systolic dysfunction from electrocardiographic images. *medRxiv*, pages 2022–06, 2022b.
- Aya Nabil Sayed, Yassine Himeur, and Fayçal Bensaali. From time-series to 2d images for building occupancy prediction using deep transfer learning. *Eng. Appl. Artif. Intell.*, 119: 105786, 2023.
- Piyush Sharma, Nan Ding, Sebastian Goodman, and Radu Soricut. Conceptual captions: A cleaned, hypernymed, image alt-text dataset for automatic image captioning. In *Annual Meeting of the Association for Computational Linguistics*, 2018.
- Luis R. Soenksen, Yu Ma, Cynthia Zeng, Léonard Boussioux, Kimberly Villalobos Carballo, Liangyuan Na, Holly M. Wiberg, Michael L. Li, Ignacio Fuentes, and Dimitris Bertsimas. Integrated multimodal artificial intelligence framework for healthcare applications. *NPJ Digital Medicine*, 5, 2022.
- Sulaiman S Somani, Adam J Russak, Felix Richter, Shan P Zhao, Akhil Vaid, Fayzan F. Chaudhry, Jessica K De Freitas, Nidhi Naik, R. Miotto, Girish N. Nadkarni, Jagat Narula, Edgar Argulian, and Benjamin S. Glicksberg. Deep learning and the electrocardiogram: review of the current state-of-the-art. *Europace*, 23:1179 – 1191, 2021.
- Yonghao Song, Xueyu Jia, Lie Yang, and Longhan Xie. Transformer-based spatial-temporal feature learning for eeg decoding. *ArXiv*, abs/2106.11170, 2021.
- Sören Richard Stahlschmidt, Benjamin Ulfenborg, and Jane Synnergren. Multimodal deep learning for biomedical data fusion: a review. *Briefings in Bioinformatics*, 23, 2022.
- Nils Strodthoff, Patrick Wagner, Tobias Schaeffter, and Wojciech Samek. Deep learning for eeg analysis: Benchmarks and insights from ptb-xl. *IEEE Journal of Biomedical and Health Informatics*, 25:1519–1528, 2021.
- Patrick Wagner, Nils Strodthoff, R. Bousseljot, D. Kreiseler, F. Lunze, W. Samek, and T. Schaeffter. Ptb-xl, a large publicly available electrocardiography dataset. *Scientific Data*, 7, 2020.

- Peng Wang, An Yang, Rui Men, Junyang Lin, Shuai Bai, Zhikang Li, Jianxin Ma, Chang Zhou, Jingren Zhou, and Hongxia Yang. Unifying architectures, tasks, and modalities through a simple sequence-to-sequence learning framework. In *ICML*, 2022.
- Zhiguang Wang and Tim Oates. Encoding time series as images for visual inspection and classification using tiled convolutional neural networks. 2014.
- Huiyi Wu, Kiran Haresh Kumar Patel, Xinyang Li, Bowen Zhang, Christoforos Galazis, Nikesh Bajaj, Arunashis Sau, Xili Shi, Lin Sun, Yanda Tao, et al. A fully-automated paper ecg digitisation algorithm using deep learning. *Scientific Reports*, 12(1):20963, 2022.
- Chen Xie, Lucas McCullum, Alistair Johnson, Tom Pollard, Brian Gow, and Benjamin Moody. Waveform database software package (wfdb) for python. *PhysioNet*.
- Jinyu Yang, Jiali Duan, S. Tran, Yi Xu, Sampath Chanda, Liqun Chen, Belinda Zeng, Trishul M. Chilimbi, and Junzhou Huang. Vision-language pre-training with triple contrastive learning. *ArXiv*, abs/2202.10401, 2022.
- Jiahui Yu, Zirui Wang, Vijay Vasudevan, Legg Yeung, Mojtaba Seyedhosseini, and Yonghui Wu. Coca: Contrastive captioners are image-text foundation models. *ArXiv*, abs/2205.01917, 2022.
- Xinzhe Yuan, Dustin Tanksley, Pu Jiao, Liujun Li, Genda Chen, and Donald C. Wunsch. Encoding time-series ground motions as images for convolutional neural networks-based seismic damage evaluation. In *Frontiers in Built Environment*, 2021.
- Chaohe Zhang, Xu Chu, Liantao Ma, Yinghao Zhu, Yasha Wang, Jiangtao Wang, and Junfeng Zhao. M3care: Learning with missing modalities in multimodal healthcare data. *Proceedings of the 28th ACM SIGKDD Conference on Knowledge Discovery and Data Mining*, 2022.
- Deyun Zhang, Shijia Geng, Yang Zhou, Weilun Xu, Guodong Wei, Kai Wang, Jie Yu, Qiang Zhu, Yongkui Li, Yonghong Zhao, et al. Artificial intelligence system for detection and screening of cardiac abnormalities using electrocardiogram images. *arXiv preprint arXiv:2302.10301*, 2023.
- Pengchuan Zhang, Xiujun Li, Xiaowei Hu, Jianwei Yang, Lei Zhang, Lijuan Wang, Yejin Choi, and Jianfeng Gao. Vinvl: Revisiting visual representations in vision-language models. *2021 IEEE/CVF Conference on Computer Vision and Pattern Recognition (CVPR)*, pages 5575–5584, 2021.
- Wei-Long Zheng, Jia-Yi Zhu, Yong Peng, and Bao-Liang Lu. Eeg-based emotion classification using deep belief networks. *2014 IEEE International Conference on Multimedia and Expo (ICME)*, pages 1–6, 2014.
- Jiacheng Zhu, Jielin Qiu, Zhuolin Yang, Douglas Weber, Michael A. Rosenberg, Emerson Liu, Bo Li, and Ding Zhao. Geoeeg: Data augmentation via wasserstein geodesic perturbation for robust electrocardiogram prediction. In *Machine Learning in Health Care*, 2022.

Appendix A. Model Parameters

Table 4: Model parameters in the experiments.

Parameters	Value	ViT-base	Value	ViT-large	Value
alpha	0.4	train batch size	16	train batch size	16
k_test	128	test batch size	16	test batch size	16
weight decay	0.05	ViT layer	4	ViT layer	10
queue size	57600	init lr	1e-5	init lr	5e-6

Appendix B. More Related Works

Machine Learning in ECG With the development of machine learning and deep learning, many works have studied the application of using advanced models in ECG. [Alfaras et al. \(2019\)](#) proposed a fully automatic and fast ECG arrhythmia classifier based on a simple brain-inspired machine learning approach known as Echo State Networks. [Mishra et al. \(2020\)](#) converted ECG paper records into a 1-D signal and generated an accurate diagnosis of heart-related problems using deep learning. [Peimankar and Puthusserypady \(2020\)](#) combined CNN and long LSTM model to detect the onset, peak, and offset of different heartbeat waveforms such as the P-wave, QRS complex, T-wave, and No wave (NW). [Aziz et al. \(2021\)](#) exploited two-event related moving-averages (TERMA) and fractional-Fourier-transform (FrFT) algorithms. [Somani et al. \(2021\)](#) proposed a review focusing on orienting the clinician towards fundamental tenets of deep learning, state-of-the-art prior to its use for ECG analysis, and current applications of deep learning on ECGs. [Qiu et al. \(2022a\)](#) used Optimal Transport to augment ECG signals to improve the disease classification robustness. [Kim et al. \(2022\)](#) proposed a ML model for real-time classification of atrial fibrillation (AF) between Paroxysmal atrial fibrillation (PAF) and Non-paroxysmal atrial fibrillation (Non-PAF). [Adedinsewo et al. \(2022\)](#) evaluated how well the AI-ECG model output obtained using digitized paper ECGs agreed with the predictions from the native digital ECGs for the detection of low ejection fraction. [Ayano et al. \(2022\)](#) summarized the achievements in ECG signal interpretation using interpretable machine learning techniques. [Qiu et al. \(2022c\)](#) used transformer architecture to classify ECG signals.

Transform Time Series Signals into Images Encoding time series data as different types of images have been explored by many studies in different areas ([Wang and Oates, 2014](#)). [Hatami et al. \(2017\)](#) used Recurrence Plots (RP) to transform time series into 2D texture images. [Kavasidis et al. \(2017\)](#) converted brain signals into images. [Martínez-Arellano et al. \(2019\)](#) proposed an approach for tool wear classification based on signal imaging. [Qiu and Zhao \(2018\)](#); [Qiu et al. \(2018c\)](#) encoded EEG signals into images to improve the performance of emotion recognition. [Garcia et al. \(2020\)](#) reviewed the signal-to-image encoding approaches found in the literature. [Barra et al. \(2020\)](#) encoded financial

time series into images to predict the future trend of the U.S. market. [Qin et al. \(2020\)](#) encoded time series of sensor data as images to retain necessary features for human activity recognition. [Bi et al. \(2021\)](#) transformed time series into images to improve the accuracy of tourism demand forecasting. [Yuan et al. \(2021\)](#) developed a new image encoding technique based on time-series segmentation (TS) to transform acceleration (A), velocity (V), and displacement (D) ground motion records into a three-channel AVD image of the ground motion event. [Sayed et al. \(2023\)](#) transformed multivariate time-series data into images for better encoding and extracting relevant features for non-intrusive occupancy detection.

Multimodal Learning in Healthcare Multimodal learning has drawn increasing attention in the past few years, many datasets and models are collected and proposed to accelerate research in this field ([Chen et al., 2020b](#); [Gan et al., 2020](#); [Li et al., 2020](#); [Zhang et al., 2021](#); [Radford et al., 2021a](#); [Liu et al., 2021](#); [Kim et al., 2021a](#); [Qiu et al., 2022b](#); [Li et al., 2021b, 2022](#); [Yang et al., 2022](#); [Dou et al., 2021](#); [Ramesh et al., 2022](#); [Qiu et al., 2023](#); [Wang et al., 2022](#); [Alayrac et al., 2022](#); [Radford et al., 2021a](#); [Qiu et al., 2022d](#); [Yu et al., 2022](#)). In healthcare applications, multimodal learning also achieved much progress ([Soenksen et al., 2022](#)), including chest x-ray classification ([Sait et al., 2021](#); [Kumar et al., 2022](#)), emotion recognition ([Qiu et al., 2018a,b](#); [Bao et al., 2019](#); [Liu et al., 2019](#)), electronic health records ([Zhang et al., 2022](#)), cardiovascular diseases ([Amal et al., 2022](#)), medical signals fusion ([Ghulam et al., 2021](#)), and so on. In addition, [Cai et al. \(2019\)](#) provided a comprehensive survey of existing multimodal techniques in healthcare systems, which included not only state-of-the-art methods but also the most recent trends in the field. [Stahlschmidt et al. \(2022\)](#) reviewed state-of-the-art biomedical data fusion approaches. [Kline et al. \(2022\)](#) summarize the studies related to multimodal machine learning in precision healthcare. [Pei et al. \(2023\)](#) investigated the performance of existing multi-modal fusion pre-training algorithms and medical multi-modal fusion methods and compared their key characteristics, such as supported medical data, diseases, target samples, and implementation performance.